Supporting Information

Characterization of Self-Assembled Metallodendrimers in Solution, in the Gas Phase, and at Air-Solid Interfaces

H. Tarik Baytekin[a], Mario Sahre[a], Alexander Rang [b], Marianne Engeser[b], Andrea Schulz [c], and Christoph A. Schalley*[,c]

[a] Bundesanstalt für Materialforschung und -prüfung (BAM), Berlin

[b] Kekulé-Institut für Organische Chemie und Biochemie der Universtät Bonn

[c] Institut für Chemie und Biochemie – Organische Chemie, Freie Universität Berlin

Christoph A. Schalley, Institut für Chemie und Biochemie – Organische Chemie, Freie Universität, Berlin, Takustr. 3, D-14195, Berlin, Germany; fax: ++49 – (0)30 – 838-55817; phone: ++49 – (0)30 – 838-52639; email: schalley@chemie.fu-berlin.de

1.1 Influence of concentration on self-assembly of 14b on HOPG.

The concentration dependence of the surface morphology of **14b** on HOPG was given in **Figure 1**. The third generation self-assembled dendrimers were drop casted from a freshly prepared acetone solution. The coverage of the surface by the dendrimer film increases with the concentration. Concentrations higher than 10 μM resulted in the formation of a continuous dendrimer film on HOPG. At lower concentrations, the average height of dendrimeric layer varies only very slightly between 0.7 and 0.9 nm irrespective of the sample concentration (Figures 1a-d). This height may correspond to the height of a monolayer on the surface. Values below 1 nm are well in line with modeling calculations of a single dendrimer, if one assumes that the contact between the aromatic subunits incorporated in the dendrons with the surface is maximized. This effect should lead to a substantial flattening of the dendritic square and thus would result in flat, oblate-shaped dendrimers that laterally interact to form the film. At this stage of the study, we decided to use the deposition on HOPG from acetone solutions as the standard protocol with which all images presented below have been generated.

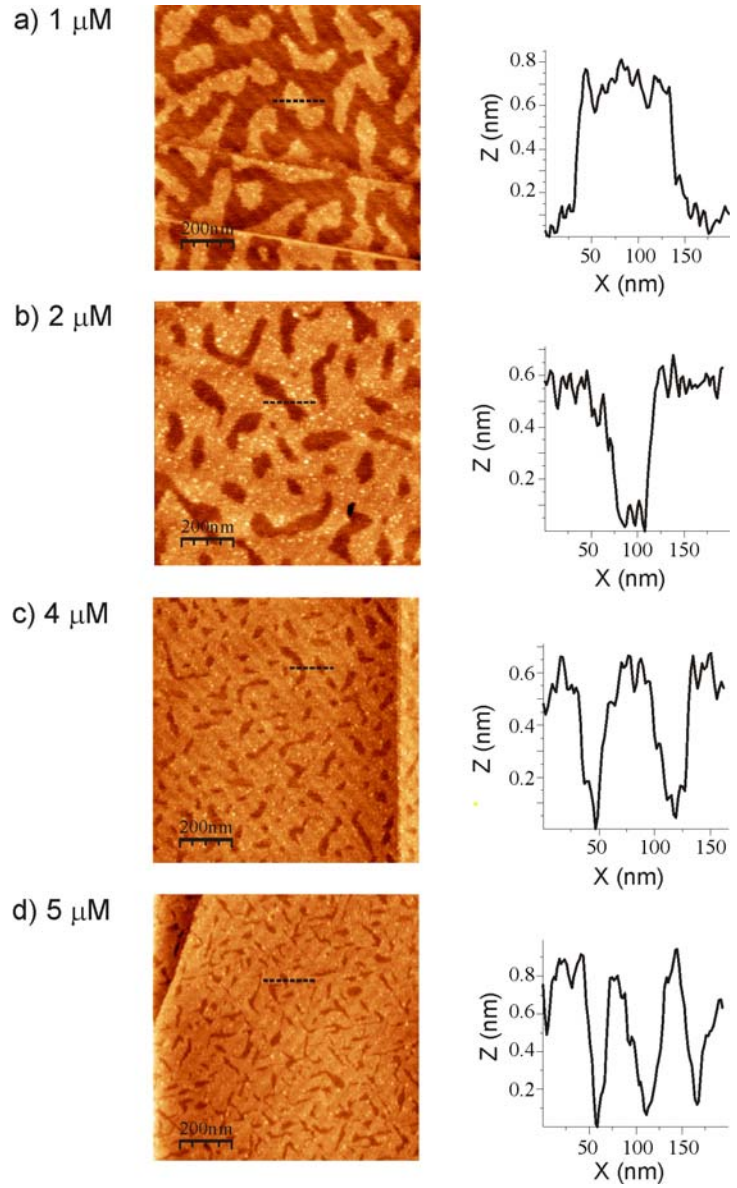

Figure S1. TM-AFM height image of **14b** on HOPG at different concentrations. Influence of concentration on surface morphology is shown by the changes in height images, (a - d), and line profiles through dendrimer aggregates (dashed lines in the height images).

1.2. Time dependent topographical changes of 13b and 14b on HOPG.

Time-dependent changes on surface topography provide more detailed insight: A series of consecutive AFM measurements that were performed using the same assembly **13b** under the same measurement conditions only at different time intervals after sample preparation are given in **Figure 2** (top). The AFM images shown in Figures 2a and 2b are obtained from the same area with a time interval of 10 minutes. Very similar dendrimer patterns were observed from a nearby area, given in Figure 2c-f. Some of the selected height profiles along the dendrimer layers of **13b** are also shown for a better understanding of the topographical

changes during the measurements. The height images that were obtained at different times revealed a formation and subsequent reorientation of worm-like assemblies on the HOPG surface as time progresses (Figures 2a to 2j). Another consequence of the mobility of the assemblies is an increase in the average height of G2 dendrimer layers, see the height profiles (i, ii, and iii) for the lines accompanying Figures 2a, c, and f, respectively. Moreover, higher aggregates appeared as brighter species (e.g. white dots in Figure 2f), above the first metallo-dendrimer layer after 132 minutes.

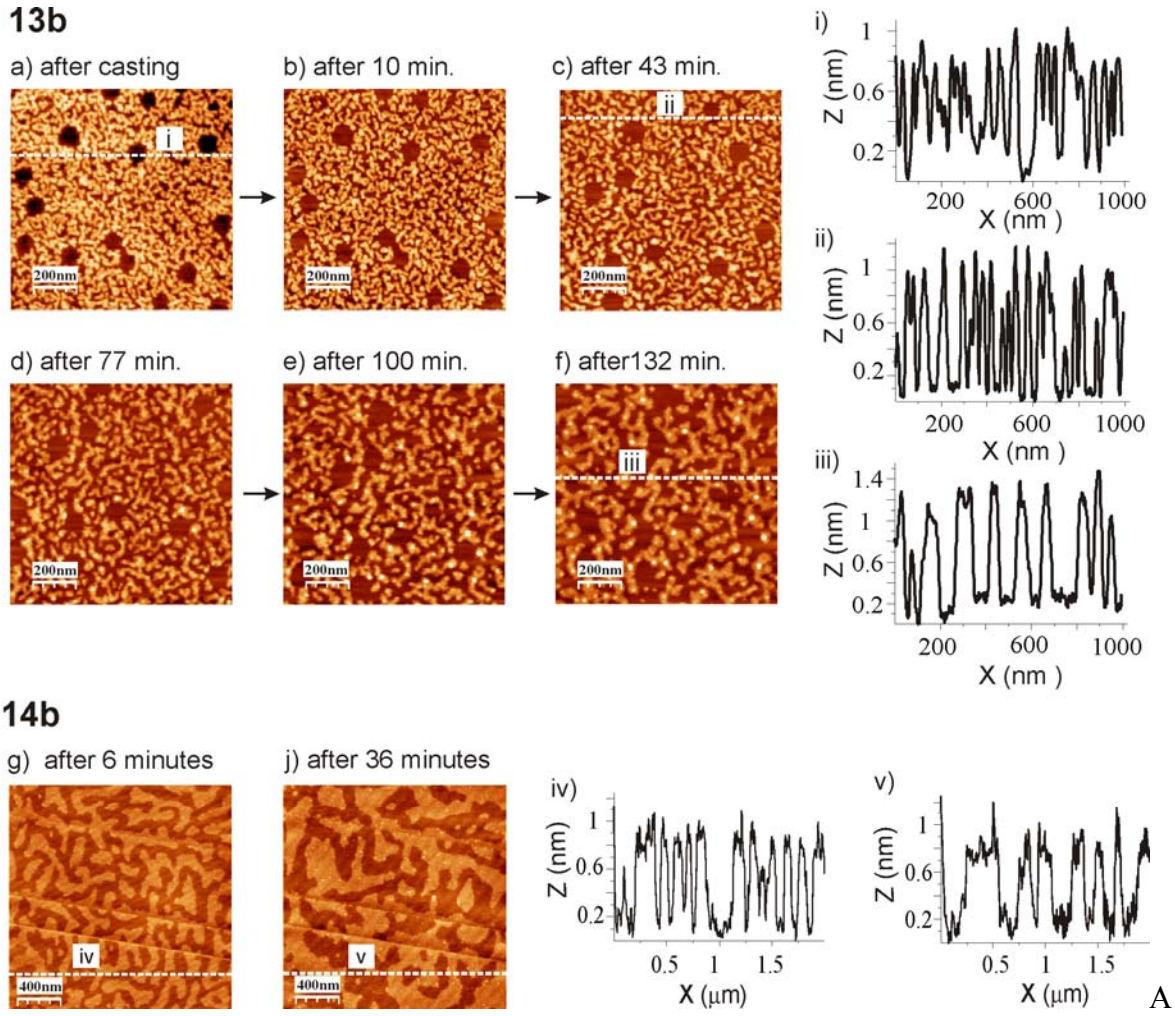

Figure S2. Time-dependent morphological changes in the height images (a - f) for **13b** (top), and (g, j) for **14b** (bottom) on HOPG. The concentrations are 2 μm for **13b** and 1μm for **14b**.

FM height images of deposited **14b** are shown in Figure 2 (bottom). Some topographical changes are observed after the preparation of the **14b** dendrimer layer on HOPG. Remarkably, some of the separated self-assembled dendrimer islands that are distributed over the HOPG surface are combined and the average height of **14b** dendrimer layer does not change much. Moreover, similar to **13b** assemblies, randomly distributed higher aggregates appeared on the

first layer after approximately 30 minutes. The topographical changes indicate that rearrangements take place which maximize the interactions between the dendrimer molecules by either combining smaller individual islands into larger ones or by increasing the height and the formation of the corresponding worm-like structures. For this process, dendrimer/dendrimer interactions are responsible.

2. Experimental Details, Syntheses and Analytical data

General methods. All reactions were conducted under a dry argon atmosphere using Schlenk techniques, unless otherwise noted. NMR spectra were acquired on Bruker DRX 500 (^{1}H (500 MHz), ^{13}C (125 MHz), ^{19}F (470 MHz), and ^{31}P (202 MHz) nuclei), DPX 400 (^{1}H (400 MHz), ^{13}C (100 MHz), ^{19}F (376 MHz), and ^{31}P (162 MHz) nuclei), or DPX 300 (^{1}H (300 MHz)) spectrometers at room temperature. All ^{1}H chemical shifts are reported in ppm relative to residual non-deuterated solvent signals as the internal standard: $CDCl_3$ (7.24 ppm), [D_6]-DMSO (2.50 ppm), [D_7]-DMF (2.75 ppm). ^{13}C chemical shifts are given in ppm relative to the carbon resonance of the deuterated NMR solvent: $CDCl_3$ (77.0 ppm), [D_6]-DMSO (39.52 ppm), [D_7]-DMF (29.76 ppm). ^{31}P chemical shifts are provided in ppm relative to external 86% H_3PO_4 (0 ppm). ^{19}F chemical shifts are reported relative to external $CFCl_3$ (0.00 ppm). Routine mass spectra were recorded on EI, FAB, and ESI mass spectrometers. Mass spectra of the squares were recorded with a Bruker APEX IV Fourier-transform ion-cyclotron resonance (FT-ICR) mass spectrometer equipped with a superconducting 7 T magnet and an Apollo ESI source. 400 μM analyte solutions in acetone were introduced into the ion source with a syringe pump (Cole Parmer Intruments, Series 74900) at flow rates of about 3 μL min^{-1}. Ion transfer into the first of three differential pumping stages in the ion source occurred through a nickel-coated glass capillary with 0.5 mm inner diameter. Typical ionization parameters were: capillary: -4.5 kV; end plate: -4.0 kV; capexit: 100 V; skimmer 1: 4.0 V; skimmer 2: 6.0 V; temperature of drying gas: 30 °C. Nitrogen was used as nebulizing gas (30 psi) and drying gas (5 psi). The ions were accumulated in a hexapole for 0.1 - 1.5 s, introduced into the FT-ICR cell operated at pressures below 10^{-10} mbar, and detected by a standard excitation and detection sequence. Short hexapole accumulation times are crucial for the smaller generation dendrimers, because they quickly decompose presumably through blackbody irradiation from the instruments walls. Larger dendrimers are capable of storing a larger amount of internal energy due to the higher number of vibrational degrees of freedom. Here, the hexapole times do not have a comparably large effect. For each measurement, 16 -

64 scans were accumulated to improve the signal-to-noise ratio. Melting points were obtained with a Büchi-SMP-20 and were not corrected.

AFM measurements were performed on two different instrument: Dimensions 3100 AFM (Digital Instruments/Veeco) and Nanoscope Multimode IIIa (Digital Instruments). WsXM 4.0 Develop 11.1 was used for imaging[5]. All images were flattened previous to height analysis using algorithms contained in the software. Tip convolution makes lateral dimension analysis difficult. NanoScope software, the influence of substrate type and concentration on surface morphology was investigated using two different AFM instruments using tapping mode AFM (TM-AFM) in both models. Measurements were performed in laboratory air at room temperature.

Model 1: The AFM measurements have been performed using a Dimensions 3100 AFM. (Digital Instruments, Veeco). Silicone probes Typ RTESP manufactured by Nanodevices with a curvature radius of >10 nm were used. Measurement scan rates were 2 - 6 μm/s during the measurements and the nominal spring constant was 20 - 80 N/m. The cantilever was forced to oscillate near resonance frequency (about 220 kHz), oscillation amplitude and control damping were adjusted to minimize tip-sample interaction. Especially after repeated (time-dependency) measurements enlarged area were imaged additionally to verify that surface movement and agglomeration of dendrimers were not tip-induced.

Model 2: The AFM measurements have been performed using a, Nanoscope Multimode IIIa (Digital Instruments, Santa Barbara, CA). The microscope was operated in the Tapping Mode using silicone probes at resonance frequencies of 150-190 KHz under ambient conditions. The cantilever was forced to oscillate near its resonance frequency. The force constant of the silicon cantilever (NCL-W) with a size of 225 μm was at 48 N/m with a curvature radius of >10 nm (NanoandMore GmbH, Wetzlar). (Goodfellow, Bad Nauheim, Germany).

Synthesis. Fréchet dendrons with benzyl bromides at their focal points,[1] 4-(3-(chlorocarbonyl)pyridin-4-yl)pyridine-3-carbonyl chloride **5**,[2] and the metal corner complexes (dppp)Pd(OTf)$_2$ and (dppp)Pt(OTf)$_2$ (**10a,b**)[3] were prepared and purified according to literature procedures. The analytical data obtained are in accordance with those reported. The conversion of the dendritic benzyl bromides into the corresponding amines (**1 – 4**) also followed procedures published earlier.[4]

3,3'-diethyl-[4,4']bipyridine: Synthesized according to the following modified procedure. The original procedure was described for 3,3'-dimethyl-4,4'-bipyridine in: J. Rebek, Jr., T. Costello, R. Wattley, *J. Am. Chem. Soc.* **1985**, *107*, 7487-7493.

In dry diethyl ether, 3-ethylpyridine (1.05 mL, 0.95 g/ml, 1.00 g, 107.2 g/mol, 9.3 mmol), chlorotrimethylsilane (1 eq.) and sodium (1.1 eq, in small portions) were added at 0 °C. The suspension was stirred over night and dried roughly. The residue is extracted with hot toluene several times until the extract is colorless. The toluene is removed and the residue is dried roughly, again. An acetone-water-mixture and solid potassium permanganate is added under stirring until the characteristic color remains. Stirring is continued for further 30 min., the solid is filtered off, washed with a warm acetone-water-mixture and the acetone is removed from the filtrate. The aqueous phase is extracted with chloroform (3 times 10 ml). After drying over sodium sulfate and removing of the solvent, the crude product was purified by flash chromatography. White solid. Yield: 194 mg, 0.9 mmol, 19 %. R_f = 0.40 EtOAc. ^{1}H NMR (400 MHz; $CDCl_3$; 298 K; Me_4Si): δ (ppm) = 8.59 (s, 2 H, H-2 and H-2'), 8.49 (d, 2 H, ^3J = 5.0 Hz, H-6 and H-6'), 7.00 (d, 2 H, ^3J = 5.0 Hz, H-5 and H-5'), 2.45 (m, 2 H, CH_2), 2.35 (m, 2 H, CH_2), 1.06 (t, 6 H, ^3J = 7.6 Hz, CH_3). ^{13}C NMR (100 MHz; $CDCl_3$; 298 K): δ (ppm) = 150.6, 147.2, 145.9, 136.5, 123.4, 23.8, 15.1. MS (EI) $M^{\cdot+}$ calc. for $C_{14}H_{16}N_2$ 212.1313 Da found 212.1311 Da (1 ppm).

General procedure for the preparation of bis-amide-substituted bipyridines (6 – 9). At 0°C, 4-(3-(chlorocarbonyl)pyridin-4-yl)pyridine-3-carbonyl chloride **5** (0.282 g, 1 mmol) was added in six portions over 1 h to a solution of the desired amine (2.5 mmol) and triethylamine 0.698 mL (5 mmol) in dry THF (50 mL). The reaction flask was allowed to reach room temperature and the reaction mixture was stirred overnight. The solvents were removed and the light yellow solid was purified by column chromatography.

4-(3-(benzylcarbamoyl)pyridin-4-yl)-N-benzylpyridine-3-carboxamide (6): White solid. Yield: 85%. R_f = 0.35. CH_2Cl_2 : MeOH = 10 : 1 (SiO_2). m.p. = 175°C. ^{1}H NMR (400 MHz; [D_7]-DMF; 298 K;Me_4Si): δ (ppm) = 9.15 (t, 2H, ^3J=5.68 Hz, H_{amide}), 8.83 (s, 2H, $H_{pyridine}$), 8.71 (d, 2H, ^3J=5.05 Hz, $H_{pyridine}$), 7.28-7.23 (m, 6H, H_{phenyl}), 7.05 (m, 6H, H_{phenyl}+$H_{pyridine}$), 4.39 (d, 4H, ^3J=5.94 Hz, $H_{benzylic}(CONCH_2)$). ^{13}C NMR (100 MHz; [D_7]-DMF; 298 K; Me_4Si): δ (ppm) = 167.1, 150.6, 148.2, 144.8, 138.7, 131.2, 128.3, 127.0, 126.8, 123.4, 42.8. MS (EI, 70 eV): m/z (%) = 422.1 (77.6) [$M^{\cdot+}$], 317.1 (15.2), 288.1 (23.2), 270.1 (6.4), 198.1 (44.8), 183.0 (88.8), 155.0 (6.8), 106.1 (96.8), 91.0 (100). MS (ESI, MeOH) [MH^+] calc. for $C_{26}H_{23}N_4O_2$ 423.1816 Da found 423.1818 Da (+0.5 ppm).

4-(3-(3,5-bis(benzyloxy)benzylcarbamoyl)pyridin-4-yl)-N-(3,5-bis(benzyloxy)benzyl)pyridine-3-carboxamide (7): White solid. Yield: 66%. R_f = 0.39. CH_2Cl_2 : MeOH = 17 : 1 (SiO_2). m.p. = 68°C. ^{1}H NMR (400 MHz; [D_7]-DMF; 298 K; Me_4Si): δ (ppm) = 9.12 (t, 2H, ^{3}J=5.92 Hz, H_{amide}), 8.81 (s, 2H, $H_{pyridine}$), 8.63 (d, 2H, ^{3}J=4.93 Hz, $H_{pyridine}$), 7.52 (m, 8H, H_{phenyl}), 7.40 (m, 8H, H_{phenyl}), 7.33 (m, 4H, H_{phenyl}), 7.24 (d, 2H, ^{3}J=5.05 Hz, $H_{pyridine}$), 6.61 (t, 2H, ^{4}J=2.15 Hz, $H_{aromatic}$), 6.50 (d, 4H, ^{4}J=2.28 Hz, $H_{aromatic}$), 5.10 (s, 8H, $H_{benzylic}(PhCH_2O)$, 4.35 (d, 4H, ^{3}J=5.94 Hz, $H_{benzylic}(CONCH_2)$). ^{13}C NMR (100 MHz; $CDCl_3$; 298 K): δ (ppm) = 166.9, 160.2, 150.9, 148.1, 144.7, 139.7, 136.8, 130.6, 128.6, 128.1, 127.6, 123.0, 106.9, 100.9, 70.1, 43.9. MS (EI, 70 eV): m/z (%) = 846.2 (25.5) [$M^{\cdot+}$], 755.1 (9.1), 527.1 (7.3), 318.1 (5.5), 228.1 (3.6), 194.1 (5.5), 168.0 (7.4), 104.0 (12.7), 91.0 (100). MS (ESI, MeOH) [MH^+] calc. for $C_{54}H_{47}N_4O_6$ 847.3490 Da found 847.3479 Da (-1.3 ppm).

4-(3-(3,5-bis(3,5-bis(benzyloxy)benzyloxy)benzylcarbamoyl)pyridin-4-yl)-N-(3,5-bis(3,5-bis(benzyloxy)benzyloxy)benzyl)pyridine-3-carboxamide (8): Pale yellow solid 81%. R_f = 0.54. CH_2Cl_2 : MeOH = 10 : 1 (SiO_2). m.p. = 70°C. ^{1}H NMR (400 MHz; [D_7]-DMF; 298 K; Me_4Si): δ (ppm) = 9.13 (t, 2H, ^{3}J=5.12 Hz, H_{amide}), 8.85 (s, 2H, $H_{pyridine}$), 8.63 (d, 2H, ^{3}J =5.06 Hz, $H_{pyridine}$), 7.50 (m, 16H, H_{phenyl}), 7.40 (m, 16H, H_{phenyl}), 7.34 (m, 8H, H_{phenyl}), 7.25 (d, 2H, ^{3}J =4.92 Hz, $H_{pyridine}$), 6.83 (d, 8H, ^{4}J=2.02 Hz, $H_{aromatic}$), 6.72 (t, 4H, ^{4}J=2.09 Hz, $H_{aromatic}$), 6.62 (b, 2H, $H_{aromatic}$), 6.48 (d, 4H, ^{4}J=1.64 Hz, $H_{aromatic}$), 5.15 (s, 16H, $H_{benzylic}(PhCH_2O)$), 5.04 (s, 8H, $H_{benzylic}(ArCH_2O)$), 4.35 (d, 4H, ^{3}J=5.68 Hz, $H_{benzylic}(CONCH_2)$). ^{13}C NMR (100 MHz; $CDCl_3$; 298 K): δ (ppm) = 166.6, 160.3, 160.0, 150.6, 147.9, 144,9, 139.6, 139.3, 136.8, 130.6, 128.6, 128.1, 127.6, 123.0, 107.0, 106.5, 101.6, 100.9, 70.2, 69.9, 43.9. MS (FAB): m/z = 1695.6 [M+H]$^+$.

4-(3-(3,5-bis(3,5-bis(3,5-bis(benzyloxy)benzyloxy)benzyloxy)benzylcarbamoyl)pyridin-4-yl)-N-(3,5-bis(3,5-bis(3,5-bis(benzyloxy)benzyloxy)benzyloxy)benzyl)pyridine-3-carboxamide (9):

Pale yellow solid. Yield: 45%. R_f = 0.54. CH_2Cl_2 : MeOH = 10 : 1 (SiO_2). m.p. = 70°C. ^{1}H NMR (400 MHz; [D_7]-DMF; 298 K; Me_4Si): δ (ppm) = 9.05 (t, 2H, ^{3}J=5.04 Hz, H_{amide}), 8.70 (s, 2H, $H_{pyridine}$), 8.50 (d, 2H, ^{3}J =5.09 Hz, $H_{pyridine}$), 7.42-7.23 (m, 80H, H_{phenyl}), 7.06 (d, 2H, ^{3}J=5.29 Hz, $H_{pyridine}$), 6.67 (m, 24H, $H_{aromatic}$), 6.58 (b, 12H, $H_{aromatic}$), 6.50 (b, 2H, $H_{aromatic}$), 6.33 (b, 4H, $H_{aromatic}$), 5.00 (s, 32H, $H_{benzylic}(ArCH_2O)$), 4.95 (s, 16H, $H_{benzylic}(PhCH_2O)$), 4.89 (s, 8H, $H_{benzylic}(ArCH_2O)$, 4.18 (b, 4H, ($H_{benzylic}(CONCH_2)$). ^{13}C NMR (100 MHz; $CDCl_3$; 298

K): δ (ppm) = 166.7, 160.2, 160.2, 160.2, 160.1, 139.6, 139.4, 139.3, 136.9, 136.8, 128.6, 128.1, 128.0, 127.6, 127.6, 106.9, 106.5, 101.7, 70.2, 70.0, 69.9, 69.6, 53.9, 43.9, 31.8, 29.4. MS (ESI, acetone) [MH^+] calc. for $C_{222}H_{191}N_4O_{30}$ 3392.3538 Da found 3392.3432 Da (-3.1 ppm).

General procedure[3] for the preparation of squares 11a,b – 14a,b. Equimolar amounts (typically 0.06 mmol) of (dppp)M$(OTf)_2$ (M = Pd, Pt) and the corresponding ligand **6** – **9** were dissolved in 25 mL of CH_2Cl_2 and the reaction mixture was stirred at 25°C for 2 h. The reaction mixture was filtered and the filtrate was reduced to half of its volume. Slow addition of diethyl ether into the reaction mixture resulted a white precipitate. Filtration of the precipitate yielded the desired products as white solids. The isolated yields are between 70 and 85 % for G0 to G2. The only exceptions from this procedure are the G3 substituted squares which did not precipitate when ether was added. They were synthesized by mixing the bipyridine ligand and the metal corner and were used without further workup.

^{13}C NMR spectra of squares 12b – 14b: Because of dynamic processes, first (**12b**), second (**13b**) and third (**14b**) generation Pt squares gave complex ^{1}H NMR spectra at room temperature. Only at high temperatures, isomer interconversions are fast enough to provide simple ^{1}H NMR spectra. To obtain interpretable ^{13}C NMR spectra, temperatures above the instrument limit would be necessary so that we cannot provide the ^{13}C NMR data for **12b – 14b**.

Square 11a: White solid. ^{1}H NMR (400 MHz; [D_7]-DMF; 298 K; Me_4Si): δ (ppm) = 9.12 (b, 8H, H_{amide}), 8.82 (s, 8H, $H_{pyridine}$), 8.74 (d, 8H, ^3J = 4.93 Hz, $H_{pyridine}$), 7.89 (m, 32H, $H_{dppp\text{-}ortho}$), 7.71 (m, 16H, $H_{dppp\text{-}para}$), 7.60 (m, 32H, $H_{dppp\text{-}meta}$), 7.25 (m, 32H, H_{phenyl}), 7.04 (m, 16H, H_{phenyl} + $H_{pyridine}$), 4.38 (d, 16H, ^3J = 5.94 Hz, $H_{benzylic}(CONCH_2)$), 3.18 (m, 16H, H_{dppp}), 2.12 (m, 8H, H_{dppp}). ^{13}C NMR (100 MHz; [D_7]-DMF; 298 K): δ (ppm) = 166.1, 151.3, 149.0, 139.1, 134.0 (b, C_{dppp}), 133.3, 130.2, 130.1, 128.9, 127.5, 127.5, 125.8 (d, $J_{P\text{-}C}$ = 58.3 Hz), 124.8 (b, C_{dppp}), 123.6, 120.4, 43.5, 22.3 (d, $J_{P\text{-}C}$ = 43.1 Hz), 18.6. ^{31}P NMR (162 MHz, [D_7]-DMF, 298 K): δ (ppm) = 18.9. ^{19}F NMR (376 MHz, [D_7]-DMF, 298 K): δ (ppm) = -78.95. MS (ESI, acetone): m/z = 2329.4 Da $[M\text{-}2OTf]^{2+}$.

Square 11b: White solid. ^{1}H NMR (400 MHz; [D_7]-DMF; 298 K; Me_4Si): δ (ppm) = 8.82 (b, 24H, H_{amide} + $H_{pyridine}$), 7.87 (m, 32H, $H_{dppp\text{-}ortho}$), 7.54 (m, 56H, $H_{dppp\text{-}para}$ + $H_{dppp\text{-}meta}$ +

H_{phenyl}), 7.24 (m, 40H, H_{phenyl}+ $H_{pyridine}$), 4.33 (m, 16H, $H_{benzylic}(CONCH_2)$), 3.21 (m, 16H, H_{dppp}), 2.31 (m, 8H, H_{dppp}). ^{13}C NMR (100 MHz; [D_7]-DMF; 298 K): δ (ppm) = 167.0, 149.3, 148.3, 139.0, 133.8, 133.0, 129.9, 129.8, 128.7, 127.3, 127.2, 124.8, 123.4, 120.2, 116.9, 43.3, 21.9, 18.4. ^{31}P NMR (202 MHz, [D_7]-DMF, 373 K): δ (ppm) = -9.79 (^{195}Pt satellites $^1J_{Pt-P}$ =3116 Hz). ^{19}F NMR (376 MHz, [D_7]-DMF, 298 K): δ (ppm) = -78.37. MS (ESI, acetone): m/z = 2506.4 Da $[M-2OTf]^{2+}$, 1621.6 Da $[M-3OTf]^{3+}$, 1179.2 Da $[M-4OTf]^{4+}$, 913.2 Da $[M-5OTf]^{5+}$.

Square 12a: White solid. ^{1}H NMR (400 MHz; [D_7]-DMF; 298 K; Me_4Si): δ (ppm) = 9.05 (b, 8H, H_{amide}), 8.85 (s, 8H, $H_{pyridine}$), 8.68 (d, 8H, ^3J = 4.08 Hz, $H_{pyridine}$), 7.89 (m, 32H, $H_{dppp-ortho}$), 7.69 (m, 16H, $H_{dppp-para}$), 7.58 (m, 32H, $H_{dppp-meta}$), 7.51 (m, 32H, H_{phenyl}), 7.44 (m, 32H, H_{phenyl}), 7.36 (m, 16H, H_{phenyl}), 7.25 (d, 8H, ^3J = 5.16 Hz, $H_{pyridine}$), 6.63 (t, 8H, ^4J = 2.22 Hz, $H_{aromatic}$), 6.49 (d, 16H, ^4J = 1.88 Hz, $H_{aromatic}$), 5.09 (s, 32H, $H_{benzylic}(PhCH_2O)$), 4.33 (d, 16H, ^3J = 5.80 Hz, $H_{benzylic}(CONCH_2)$), 3.18 (m, 16H, H_{dppp}), 2.26 (m, 8H, H_{dppp}). ^{13}C NMR (100 MHz; [D_7]-DMF; 298 K): δ (ppm) = 165.7, 160.4, 151.2, 148.7, 141.3, 137.7, 133.7, 133.0, 129.9, 129.8, 128.8, 128.2, 128.1, 125.6 (d, J_{P-C} = 59.3 Hz), 124.9, 123.4, 120.2, 106.9, 100.4, 70.0, 43.4, 22.1 (d, J_{P-C} = 42.9 Hz), 18.4. ^{31}P NMR (162 MHz, [D_7]-DMF, 298 K): δ (ppm) = 18.90. ^{19}F NMR (282 MHz, [D_7]-DMF, 298 K): δ (ppm) = -78.15. MS (ESI, acetone): m/z = 3177.3 Da $[M-2OTf]^{2+}$, 2069.5 Da $[M-3OTf]^{3+}$.

Square 12b: White solid. ^{1}H NMR (400 MHz; [D_7]-DMF; 298 K; Me_4Si): δ (ppm) = 8.83 (b, 8H, $H_{pyridine}$), 8.64 (b, 16H, $H_{pyridine}$ + H_{amide}), 7.86 (b, 32H, $H_{dppp-ortho}$), 7.62 (b, 16H, $H_{dppp-para}$), 7.54 (b, 32H, $H_{dppp-meta}$), 7.45 (b, 32H, H_{phenyl}), 7.38 (b, 32H, H_{phenyl}), 7.32 (b, 16H, H_{phenyl}), 7.18 (b, 8H, $H_{pyridine}$), 6.62 (b, 8H, $H_{aromatic}$), 6.50 (b, 16H, $H_{aromatic}$), 5.09 (b, 32H, $H_{benzylic}(PhCH_2O)$), 4.28 (b, 16H, $H_{benzylic}(CONCH_2)$), 3.19 (b, 16H, H_{dppp}), 2.31 (b, 8H, H_{dppp}). ^{31}P NMR (202 MHz, [D_7]-DMF, 373 K): δ (ppm) = -9.76, (^{195}Pt satellites $^1J_{Pt-P}$ = 3286 Hz). ^{19}F NMR (470 MHz, [D_7]-DMF, 298 K): δ (ppm) = -79.03. MS (ESI, acetone): m/z = 3355.1 Da $[M-2OTf]^{2+}$, 2187.6 Da $[M-3OTf]^{3+}$.

Square 13a: White solid. ^{1}H NMR (400 MHz; [D_7]-DMF; 298 K; Me_4Si): δ (ppm) = 9.06 (b, 8H, H_{amide}), 8.85 (b, 8H, $H_{pyridine}$), 8.68 (d, 8H, ^3J = 4.68 Hz, $H_{pyridine}$), 7.89 (m, 32H, $H_{dppp-ortho}$), 7.69 (m, 16H, $H_{dppp-para}$), 7.58 (m, 32H, $H_{dppp-meta}$), 7.49 (m, 64H, H_{phenyl}), 7.40 (m, 64H, H_{phenyl}), 7.36 (m, 32H, H_{phenyl}), 7.24 (d, 8H, ^3J = 5.05 Hz, $H_{pyridine}$), 6.82 (d, 32H, ^4J = 2.15 Hz, $H_{aromatic}$), 6.71 (t, 16H, ^4J = 2.21 Hz, $H_{aromatic}$), 6.63 (t, 8H, ^4J = 1.96, $H_{aromatic}$), 6.48 (d, 16H, ^4J = 1.77, $H_{aromatic}$), 5.14 (s, 64H, $H_{benzylic}(PhCH_2O)$, 5.04 (s, 32H, $H_{benzylic}(ArCH_2O)$, 4.33 (d,

16H, ^{3}J=5.68 Hz, $H_{benzylic}(CONCH_2)$), 3.16 (m, 16H, H_{dppp}), 2.25 (m, 8H, H_{dppp}). ^{13}C NMR (100 MHz; [D_7]-DMF; 298 K): δ (ppm) = 166.6, 160.5, 160.3, 151.0, 148.6, 141.4, 140.2, 137.7, 133.8 (b, C_{dppp}), 133.1, 129.9, 128.8, 128.3, 128.2, 128.1, 125.5 (d, J_{P-C} = 56.9 Hz), 123.4, 120.2, 107.0, 106.9, 101.5, 100.6, 70.1, 69.9, 43.5, 22.1 (d, J_{P-C} = 43.5 Hz), 18.6. ^{31}P NMR (162 MHz, [D_7]-DMF, 298 K): δ (ppm) = 19.02. ^{19}F NMR (376 MHz, [D_7]-DMF, 298 K): δ (ppm) = -79.11. MS (ESI, acetone): m/z = 4876.7 Da $[M\text{-}2OTf]^{2+}$, 3200.9 Da $[M\text{-}3OTf]^{3+}$.

Square 13b: White solid. ^{1}H NMR (400 MHz; [D_7]-DMF; 298 K; Me_4Si): δ (ppm) = 8.83 (b, 8H, $H_{pyridine}$), 8.62 (b, 16H, $H_{pyridine}$ + H_{amide}), 7.85 (b, 32H, $H_{dppp\text{-}ortho}$), 7.54 (b, 48H, $H_{dppp\text{-}para}$+$H_{dppp\text{-}meta}$), 7.44 (b, 64H, H_{phenyl}), 7.36 (b, 64H, H_{phenyl}), 7.30 (b, 32H, H_{phenyl}), 7,16 (b, 8H, $H_{pyridine}$) 6.78 (s, 32H, $H_{aromatic}$), 6.70 (s, 16H, $H_{aromatic}$), 6.62 (s, 8H, $H_{aromatic}$), 6.49 (m, 16H, $H_{aromatic}$), 5.12 (s, 64H, $H_{benzylic}(PhCH_2O)$), 5.03 (s, 32H, $H_{benzylic}(PhCH_2O)$), 4.29 (s, 16H, $H_{benzylic}(CONCH_2)$), 3.16 (s, 16H, H_{dppp}), 2.29 (m, 8H, H_{dppp}). ^{31}P NMR (202 MHz, [D_7]-DMF, 298 K): δ (ppm) = -8.32 (^{195}Pt satellites $^{1}J_{Pt\text{-}P}$ = 3237 Hz). ^{19}F NMR (470 MHz, [D_7]-DMF, 298 K): δ (ppm) = -78.87. MS (ESI, acetone): m/z = 5053.9 Da $[M\text{-}2OTf]^{2+}$, 3318.8 Da $[M\text{-}3OTf]^{3+}$.

Square 14a: ^{1}H NMR (400 MHz; [D_7]-DMF; 298 K; Me_4Si): δ (ppm) = 9.01 (b, 8H, H_{amide}), 8.70 (s, 8H, $H_{pyridine}$), 8.56 (d, 8H, ^{3}J = 4.44 Hz, $H_{pyridine}$), 7.75 (m, 32H, $H_{dppp\text{-}ortho}$), 7.60 (m, 16H, $H_{dppp\text{-}para}$), 7.50 (m, 32H, $H_{dppp\text{-}meta}$), 7.37-7.24 (m, 320H, H_{phenyl}), 7.08 (d, 8H, ^{3}J=5.04 Hz, $H_{pyridine}$), 6.66 (m, 96H, $H_{aromatic}$), 6.58 (m, 48H, $H_{aromatic}$), 6.51 (b, 8H, $H_{aromatic}$), 6.34 (b, 16H, $H_{aromatic}$), 5.00 (b, 128H, $H_{benzylic}(PhCH_2O)$), 4.95 (b, 64H, $H_{benzylic}(ArCH_2O)$, 4.89 (b, 32H, $H_{benzylic}(ArCH_2O)$, 4.18 (s, 16H, ($H_{benzylic}(CONCH_2)$), 2.88 (m, 16H, H_{dppp}), 1.92 (m, 8H, H_{dppp}). ^{13}C NMR (100 MHz; [D_6]-DMSO; 298 K): δ (ppm) = 161.9, 159.5, 159.5, 159.4, 148.3, 148.0, 140.7, 139.3, 136.8, 136.5, 133.3, 132.6, 129.2, 128.3, 127.7, 127.6, 125.9, 106.5, 106.2, 101.1, 73.5, 69.3, 69.1, 47.9, 24.9, 17.7. ^{31}P NMR (162 MHz, [D_6]-DMSO, 298 K): δ (ppm) = 19.98. ^{19}F NMR (376 MHz, [D_6]-DMSO, 298 K): δ (ppm) = -78.13.

Square 14b: ^{1}H NMR (400 MHz; [D_7]-DMF; 298 K; Me_4Si): δ (ppm) = 8.81 (b, 8H, $H_{pyridine}$), 8.56 (b, 16H, $H_{pyridine}$ + H_{amide}), 7.85 (b, 32H, $H_{dppp\text{-}ortho}$), 7.65 (b, 16H, $H_{dppp\text{-}para}$), 7.56 (b, 32H, $H_{dppp\text{-}meta}$), 7.43-7.28 (b, 320H, H_{phenyl}), 7.11 (m, 8H, $H_{pyridine}$), 6.86 –6.52 (m, 168H, $H_{aromatic}$), 5.10 (b, 128H, $H_{benzylic}(PhCH_2O)$), 5.06 (b, 64H, $H_{benzylic}(PhCH_2O)$), 5.00 (b, 32H, $H_{benzylic}(PhCH_2O)$), 4.29 (b, 16H, $H_{benzylic}(CONCH_2)$), 3.14 (m, 16H, H_{dppp}), 2.28 (m,

8H, H_{dppp}). ^{31}P NMR (202 MHz, [D_7]-DMF, 373 K): δ (ppm) = -9.19 (^{195}Pt satellites $^{1}J_{Pt-P}$ = 3237 Hz). ^{19}F NMR (470 MHz, [D_7]-DMF, 298 K): δ (ppm) = -78.16.

References

[1] a) C. J. Hawker, J. M. J. Fréchet, *J. Am. Chem. Soc.* **1990**, *112*, 7638-7647; b) C. J. Hawker, J. M. J. Fréchet, *J. Chem. Soc., Chem. Commun.* **1990**, 1010-1013.

[2] P. D. Beer, C. Zheng, G. Alan, H. Jane, *J. Chem. Soc., Chem. Commun*. **1994**, *20*, 2413-2414.

[3] P. J. Stang, D. H. Cao, S. Saito, A. M. Arif, *J. Am. Chem. Soc.* **1995**, *117*, 6273-6283.

[4] a) F. Vögtle, M. Plevoets, G. Nachtsheim, U. Wörsdörfer, *J. Prakt. Chem.* **1998**, *340*, 112-121; b) M. Luostarinen, T. Partanen, C. A. Schalley, K. Rissanen, *Synthesis,* **2004**, 255-262.

[5] Examples for dynamic ligand exchange: Hiraoka, S.; Shiro, M.; Shionoya, M. *J. Am. Chem. Soc.,* **2004**, *126*, 1214-1218. Dumitru, F.; Petit, E.; Lee, A. van der.; Barboiu, M. *Eur. J. Inorg. Chem.*, **2005**, 4225-4262. Park, S. J.; Shin, D. M.; Sakamoto, S.; Yamaguchi, K.; Chun, Y. K.; Lah, M. S.; Hong, J.-I. *Chem. Eur. J.,* **2005**, *11*, 235-241; Albrecht, M.; Mirtschin, S.; Groot, M. De.; Janser, I.; Runsink, J.; Raabe, G.; Kogej, M.; Schalley, C. A.; Fröhlich, R. *J. Am. Chem. Soc.* **2005**, *127*,10371-10387.

[6] I. Horcas, R. Fernández, J. M. Gómez-Rodríguez, J. Colchero, J. Gómez-Herrero, A. M. Baro, *Rev. Sci. Instrum*. **2007**, *78*, 013705.